Palaeogeography, Palaeoclimatology, Palaeoecology xxx (2013) xxx–xxx

Contents lists available at SciVerse ScienceDirect

Palaeogeography, Palaeoclimatology, Palaeoecology

journal homepage: www.elsevier.com/locate/palaeo

Changing environmental conditions in recent past — Reading through the study of geochemical characteristics, magnetic parameters and sedimentation rate of mudflats, central west coast of India

Ksh. Tomchou Singh [b], G.N. Nayak [a,*], Lina L. Fernandes [a], D.V. Borole [c], N. Basavaiah [d]

[a] Department of Marine Sciences, Goa University, Goa-403206, India
[b] Atomic Mineral Division, Bangalore, India
[c] Rted. Scientist National Institute of Oceanography, Goa, India
[d] Indian Institute of Geomagnetism, New Panvel, Navi Mumbai-410218, India

ARTICLE INFO

Article history:
Received 24 April 2012
Received in revised form 6 March 2013
Accepted 11 April 2013
Available online xxxx

Keywords:
Metals
Magnetic susceptibility
Sedimentation rate
Estuary
Creek

ABSTRACT

Geochemical (sediment components, major and trace metals), magnetic related parameters (concentration, mineralogy and grain size) and radionuclide (^{210}Pb) analyses were carried out on sediment cores collected from mudflat regions of central west coast of India viz, Kolamb creek (Malvan), Mandovi estuary (Panaji) and Tadri creek (Gokarn), in order to study the variations in sediment characteristics with time. The changes in spatial and temporal (depth) distributions of sediment composition were observed to be mainly controlled by the catchment area geology, geomorphology and anthropogenic activities. The sedimentation rate in the study area varied from 0.13 to 2 cm/yr. The rate was extremely low at the lower half of the cores (0.13–0.31 cm/yr, before ~1980) as compared to the near surface (1.21–2 cm/yr, after ~1980) with two clear phases of sedimentation rates. The higher sedimentation rate in the upper portions of the cores was found to correspond to increased deposition of finer sediment components, metals and magnetic minerals which in turn were found to be mainly controlled by geology and/or human activities. The results of the present study reveal variations in sediment properties with time and support the use of geochemical in addition to magnetic susceptibility parameters on mudflats to understand changing environmental conditions of recent past.

1. Introduction

The intertidal areas of coastal zones such as estuaries, creeks and bays are major sites of rapid sedimentation and accumulation of anthropogenic pollutants into their sediments. These are highly dynamic systems which are constantly influenced by local energy levels (Swart, 1983) and are prone to contamination from both land and sea-based anthropogenic activities and artificial disturbance or natural reworking of contaminated sediments. A number of studies involving the mudflat regions have been recently carried out (Fernandes and Nayak, 2009; Singh and Nayak, 2009; Fernandes and Nayak, 2010, 2012a, 2012b) wherein pollution and depositional environments have been studied using grain-size, organic matter and metals as the geochemical indicators of the environmental change. In the present study, in addition to geochemistry, the research includes response of magnetic parameters in the environment to historical pollution, with changing sedimentation rates.

Magnetic mineral analyses have been successfully used to investigate into depositional environment, sediment fluxes and sediment sources and their paleoclimatic and paleoenvironmental associations (Bloemendal et al., 1992; Stoner et al., 1995; Maher and Thompson, 1999). Combined analysis of chemical and magnetic data has proved the close relationship between magnetic susceptibility and heavy metal concentrations in marine and river sediments (Chan et al., 1998; Desenfant et al., 2004; Zhang et al., 2011) and soils (Petrovský et al., 2001). Magnetic measurements as a proxy for industrial contamination, heavy metal, petroleum hydrocarbons and polycyclic aromatic hydrocarbons in coastal environment have also been employed (Alagarsamy, 2009; Dessai et al., 2009; Rijal et al., 2010; Sangode et al., 2010; Blaha et al., 2011; Venkatachalapathy et al., 2011). Compared with most environmental archives, coastal sediments provide favorable conditions for the preservation of magnetic minerals and historical pollution records. This is because marine sedimentation is usually a reasonably continuous and steady process and the sediment layers can be dated by fallout radionuclides such as ^{210}Pb and ^{137}Cs to establish a reliable sediment chronology. Very few studies have dealt with sedimentation rates on the coastal areas of India and these are restricted to the shelf region off major rivers such as Narbada and Tapti (Borole et al., 1982;

* Corresponding author. Tel.: +91 832 6519059 (O), +91 832 2458468 (R), +91 982 2725032 (M); fax: +91 832 2451184.
E-mail addresses: nayak1006@rediffmail.com, gnnayak@unigoa.ac.in (G.N. Nayak).

0031-0182/$ – see front matter © 2013 Elsevier B.V. All rights reserved.
http://dx.doi.org/10.1016/j.palaeo.2013.04.008

Borole, 1988) on the west coast and the Godavari (Kalesha et al., 1980) on the east coast. Karbassi (1989) has dated a core from the continental shelf off Mulki (about 30 km north of Mangalore) and Manjunatha and Shankar (1992) have measured sedimentation rates on the continental shelf off Mangalore. Nigam et al. (1991) have dated sediment core from the near-shore area off Karwar, Sharma et al. (1994) have measured sedimentation rates in the near-shore and estuarine sediments off Bombay, India while a recent study by Fernandes et al. (2011) involved dating creek sediments along the coast of Mumbai. With this background, the present study was carried out with the objective of understanding the environmental changes through the investigation of sedimentological, geochemical and magnetic characteristics of sediment cores collected along the central west coast of India. Also, an attempt has been made to determine the sedimentation rates in mudflats of estuarine and creek regions in order to study the regional sedimentation pattern along the central west coast of India as there are only a limited number of studies that have tried to resolve these relationships.

2. Materials and methods

2.1. Study area

Kolamb creek (Malvan)

Malvan coast, in Maharashtra, lies at latitude 15°58′ N and longitude 73°30′ E and forms part of the Western Ghats where the Sahyadri ranges gradually meet the Arabian Sea. The coast is developed on a basement of basalt flows of the Deccan volcanic province (Kumaran et al., 2004). The overlying Tertiary formations comprise submarine fossiliferrous sediments, while Quaternary formations include soils, alluvia, laterites and littoral deposits. The laterites are underlain by clays, sandstones and lignites, and carbonaceous/gray-bluish clays occur sporadically along the Konkan Coast. The climate of the region is generally warm and moderately humid. The annual average rainfall is around 2275 mm.

Mandovi River (Panaji)

The Mandovi River, in Goa, lies at latitudes 15°09′ N and longitudes 73°45′ E and is about 70 km long fed by monsoon precipitation and discharges from a catchment area of about 1150 km^2. Its basin covers an area of about 1530 km^2 and constitutes 42% of the total land area of the Goa state. Mining activities in the catchment area and reckless construction have accelerated coastal pollution and erosion. The climate of the region is generally warm and humid and is dependent on monsoon season (June to September). It receives an average rainfall of 3000 mm. The Mandovi River drains through the Western Ghats, which is part of the Western Dharwar Craton (WDC) of Meso-archaean age. The WDC is predominantly made up of greenstone belts and tonalite–trondhjemite gneisses and is characterized by high-Mg basalts and komatites with metavolcanics and meta-sedimentary rocks. The main constituents are mafic and ultramafic volcanic rocks, arenites, phyllites, polymictic and oligomictic conglomerates, graywackes, banded iron formations and carbonates (Naqvi, 2005).

Tadri creek (Gokarn)

The Tadri River (total length 121 km), in Karnataka, lying at latitude 14°32′ N and longitude 74°21′ E, in Gokarn, rises at Manjuguni near Sirsi and after winding a westerly course of about 70 km, flows into the Arabian Sea. It has two sources, the Bakurhole rising in a pond at Manjuguni about 25 km west of Sirsi and the Donihalla whose source is close to Sirsi. The area is characterized by high humidity nearly all the year round in the coastal strip and in the Western Ghats region. The average annual rainfall is 3500 mm. Geologically, the area consists of rock formation of Archean complex which are divided into an older group of Dharwar system and a younger group termed Peninsular Gneisses. Both the Dharwar and the Peninsular Gneisses are frequently overlain by a capping of laterite which is the source of iron and manganese ores.

2.2. Sampling and analytical procedures

Three shallow cores with lengths varying from 60 to 76 cm were collected by using a hand driven PVC coring tube (1.5 m * 6 cm) from different mudflat regions (Fig. 1) i.e. Kolamb (60 cm-MAA), Mandovi (76 cm-MR) and Tadri (66 cm-GH), along the central west coast of India. The cores were recorded for visual color variations, sub-sampled at 2 cm intervals, transferred to clean polyethylene bags, stored in an icebox and transported to laboratory. The subsamples were later dried at 60 °C and homogenized. Sediment component (sand, silt, clay) analysis was carried out by Pipette method (Folk, 1968) while Organic Carbon (OC) was estimated by wet oxidation method (Gaudette et al., 1974). Sediment samples for major and trace metal analyses were digested using HF–$HClO_4$–HNO_3 mixture in teflon beakers (Jarvis and Jarvis, 1985). The final solution was analyzed for major elements and trace metals (Al, K, Mg, Ca, Fe, Mn, Co, Cr, Pb, Zn and Cu) by Atomic Absorption Spectrophotometer (GBC 932 AA). The instrument was calibrated by running blank and standard solutions prior to each element analysis. Recalibration check was performed at regular intervals. Precision was monitored by analyzing some selected samples in triplicate and was generally found to be <6% standard deviation (% SD) for the major and trace elements. Accuracy of the method was determined by comparing certified sediment standard from Geological Society of Japan (GSJ-JSd-1) with the observed values and the percentage recovery was ±97% for Zn; ±94% for Fe and Mg; ±90% for Mn, Al, Ca, K; ±85% for Cu, Pb and ± 70% for Co and Cr of the working values quoted.

Magnetic susceptibility measurements (χ) with both the high (4.7 kHz) and low (0.47 kHz) frequency measurements were performed on bulk samples using a dual frequency Bartington magnetic susceptibility meter with MS2B sensor. χ indicates the contents of all kinds of magnetic minerals. Anhysteretic Remanence Magnetization (ARM) was imparted in a steady 0.05 mT field superimposed over decreasing Alternating Field (A.F.) from 100 mT to 0 mT using a Molspin A.F. demagnetizer. ARM created within the sample was then measured using Molspin spinner magnetometer. Isothermal Remanent Magnetization (IRM) was acquired by first exposing the samples to a series of successively larger fields along one direction and then in the opposite direction (backfields, −20 mT, −30 mT, −40 mT, −100 mT, −200 mT and −300 mT) using a Pulse magnetizer (Magnetic measurements Ltd). The

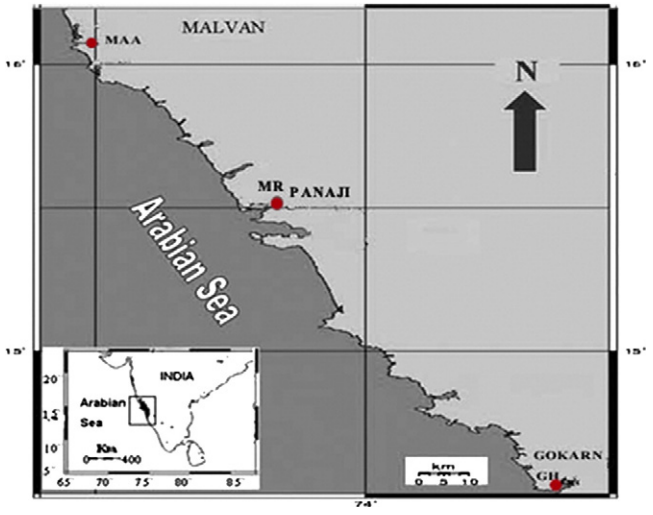

Fig. 1. Map showing the sampling locations.

IRM achieved at 2 T is referred to as the Saturation Isothermal Remanent Magnetization (SIRM). SIRM indicates the content of all magnetic particles they could get and keep remanence (Oldfield and Yu, 1994). The results were then used to calculate mass specific magnetic parameters and inter-parameter ratios such as S_{300}, χ_{fd}%, $Soft_{IRM}$ and $Hard_{IRM}$. S_{300} can be explained as the relative proportion of incomplete antiferromagnetic minerals (hematite, goethite) and ferrimagnetic minerals. The percent frequency-dependent susceptibility (χ_{fd}%) is a good indicator for the relative contribution of the pedogenic ferrimagnetic minerals to the total magnetic fraction in soil (Jordanova et al., 2008). $Soft_{IRM}$ is a measure of the concentration of ferrimagnetic minerals mostly magnetite while $Hard_{IRM}$ is a measure of the concentration of anti-ferromagnetic minerals (hematite and goethite). Temperature-dependence of magnetic susceptibility was measured for selected samples using Barrington temperature susceptibility in air, to clarify the magnetic mineral phase system. The ^{210}Pb activity was measured via its daughter nuclide ^{210}Po following the standard radiochemical procedure of Flynn (1968). Statistical analysis involving Pearson's correlation and Factor analysis was carried out with Statistica 6.0 software.

3. Results

3.1. Sediment components (sand, silt, clay and organic carbon)

In core MAA, sand, silt, clay and organic carbon (OC) ranges from 6.68 to 58.93%, 7.87 to 36.76%, 29.68 to 56.96% and 1.38 to 11.89% with average values of 30.98%, 21.89%, 47.13% and 4.96%, respectively, and the profiles show three distinct sections (Fig. 2A). The lower section (S1; 60–32 cm) is characterized by increasing trend of sand and decreasing trends of silt, clay and OC. The middle section (S2; 32–18 cm) is characterized by an erratic trend but with a lesser degree of variation of all the parameters. In the upper section (S3; 18–0 cm), sand shows a gradually decreasing trend which is compensated by increasing trends of silt and clay while an increasing trend is seen for OC. Although, the overall distribution of OC is quite similar to those of silt and clay, it shows a moderate correlation with clay which may be probably because of the extraordinarily high values of OC in the lower section of the core. It is worth mentioning here that below 32 cm, OC content increases and suddenly reaches >11% below 52 cm. In core MR, the data obtained exhibits a range from 6.14 to 27.09% for sand, 24.19 to 63.68% for silt, 24.8 to 59.12% for clay and 1.62 to 5.75% for OC with average values of 15.46%, 41.62%, 43.35% and 3.85%, respectively. From the bottom to 8 cm (Fig. 2B), sand shows a fluctuating decreasing trend with two increased peaks seen at 58 and 26 cm depths. Silt and clay, on the other hand, exhibit corresponding opposite trends with silt increasing and clay decreasing in the lower portion of the core (76–28 cm). Above 28 cm, clay shows an increasing trend towards the surface while silt increases till 8 cm and then decreases at the surface. The OC shows a decreasing trend from the bottom to the surface of the core. In core GH, sand, silt and clay data ranges from 3.04 to 19.92%, avg. 10.63%; 28.20 to 57.19%, avg. 42% and 29.68 to 60.32, avg. 47.32% respectively. OC ranges from 1.26 to 4.92% with an average of 3.08%. The sediment is found to be muddy with an average value of 89.28% mud (silt and clay). The core (Fig. 2C) can be divided into two distinct zones, the lower portion (S1; 66–52 cm) wherein the decrease in clay content is compensated by the increase in sand percentage and an upper portion (S2; 52–0 cm) where sand and silt decreases at the expense of clay. The OC projects a nearly constant trend in the lower portion and then suddenly increases at 50 cm followed by a decreasing trend in the upper portion.

3.2. Metal geochemistry

The range with mean values of the different metals analyzed is given in Table 1. In core MAA (Fig. 3A), Fe and Mn show erratic trends from the bottom to 18 cm depth, wherein enriched values are observed, probably indicating oxidized conditions resulting from the formation of oxyhydroxides. The vertical distribution of Zn is nearly uniform with depth except at the bottom of the core where a peak is seen; while Cu, Co, Cr and Pb, like Fe, exhibit increasing and decreasing trends. Among the metals analyzed Cu, Co, Cr and Al show enrichment towards the surface, especially in the upper portion of the core. Ca shows a constant trend from the bottom to 30 cm depth and above it an increasing trend is observed till the surface, suggesting dissolution of $CaCO_3$ caused by the acidic nature of the

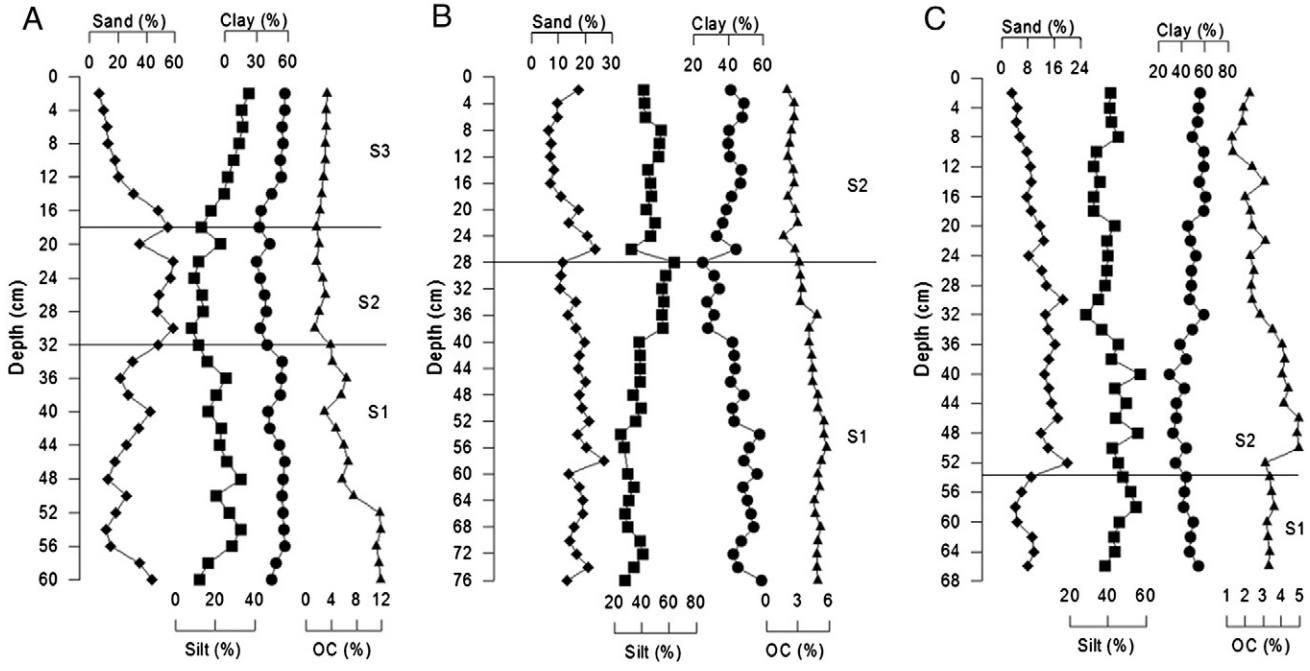

Fig. 2. Down core variation of sediment components: A — core MAA, B — core MR and C — core GH.

Table 1
Range and mean concentration of metals in the different cores studied.

Elements	Core MAA		Core MR		Core GH	
	Range	Mean ± SD	Range	Mean ± SD	Range	Mean ± SD
Fe (%)	4.99–10.08	7.34 ± 1.36	5.81–19.91	11.29 ± 4.77	6.03–7.92	6.90 ± 0.62
Mn (μg/g)	312–512	409 ± 46	825–4987	2035 ± 1377	362–574	431 ± 57
Zn (μg/g)	36.75–186	59 ± 26	64–125	81 ± 11.41	56–78	66 ± 5.81
Cu (μg/g)	55–105	74 ± 13	64–96	74 ± 7.04	42–79	51 ± 7.55
Cr (μg/g)	89–165	128 ± 20	183–303	240 ± 28.77	118–295	188 ± 40
Co (μg/g)	71–111	90 ± 8.88	28.25–194	84 ± 36.70	12.50–44	28 ± 8.03
Pb (μg/g)	13.5–113	47 ± 18.90	55–96	76 ± 11.67	0.75–30.75	18 ± 8.68
K (%)	0.54–0.91	0.69 ± 0.09	0.80–1.14	0.96 ± 0.07	1.01–1.21	1.14 ± 0.07
Mg (%)	0.31–1.32	0.69 ± 0.32	1–3.12	1.56 ± 0.33	0.80–1.75	1.33 ± 0.21
Ca (μg/g)	86–2675	927 ± 926	244–1300	534 ± 223	169–11500	2569 ± 3152
Al (%)	3.23–5.88	4.37 ± 0.71	5.61–10.45	8.33 ± 1.15	2.67–7.80	5.84 ± 1.04

SD — standard deviation.

porewaters of oxic zone of the sediments (Froelich et al., 1979). A similar trend is also observed for Mg. The significant peaks of Fe and Mn at 32 cm depth, may suggest the onset of permanently reducing conditions in agreement with Ca and most of the metal profiles and the transition of brown to gray color observed in the field.

In core MR, Al profile shows a decreasing trend from the bottom to 58 cm followed by a gradual increasing trend towards the surface (Fig. 3B). Mg shows a constant trend from the bottom to the surface except for a peak at 16 cm depth, while K maintains a constant trend throughout the core but with some minor fluctuations. On the other hand, Fe and Mn show nearly constant trends from the bottom to 32 cm depth followed by enriched and increasing trends in the upper portion (32–0 cm) of the core. Cu, Pb, Cr and Ca show fluctuating trends throughout the core. Zn, shows a constant trend except for two increased peaks at 68 and 50 cm depths. The peak at 68 cm interestingly coincides with the peak of the clay component while at 50 cm it coincides with silt peak. Zn, Cu, Cr and Pb show broadly similar distributions with depth indicating that they must be derived from the same source and/or have undergone similar post depositional behavior. The concentrations of these elements are significantly higher in the lower portion of the core except for Pb, where the OC content is also found to be higher than the overlying portion of the core.

In core GH (Fig. 3C), Al shows a decreasing trend with high values, from the bottom to 54 cm depth followed by a constant trend till 18 cm while a highly fluctuating trend but with low values, characterizes the upper portion (18–0 cm). K shows a nearly constant trend throughout the core while Mg shows an erratic trend in the bottom portion (66–48 cm) followed by a decreasing trend with minor variations up to 34 cm. Further above, an increasing trend is seen till the surface. Ca, on the other hand, shows an enriched lower portion (66–46 cm) with spikes of high values in between and an almost constant trend in the upper portion (46–0 cm). The concentration of Fe decreases from the bottom of the core to 44 cm from where it increases up to 8 cm and then decreases towards the surface. Mn, Zn and Cu show decreasing trends from the bottom to 44 cm and then gradually increase till 6 cm depth followed by a decrease towards the surface. Cr shows a decreasing trend from the bottom to 52 cm and then an increasing trend till 28 cm, above which an erratic trend is seen till the surface. Co shows a more or less increasing trend from the bottom to the surface while Pb exhibits fluctuations throughout the core length. The decrease of K/Al ratio from 54 cm to the bottom is accompanied by a sudden decrease but relatively high values of OC, Ca and Mg, which probably indicates a comparatively more marine input in addition to the diagenetic precipitation. The sudden increase of OC at 50 cm depth followed by a decreasing trend towards the surface, as also seen for Ca and Mg, may again signify the more terrigenous input modified by diagenesis.

3.3. Magnetic parameters

A similarity is observed in the profiles of the magnetic parameters in all the three cores (Fig. 4). In these cores, the concentration dependent magnetic parameters (χ, χ_{ARM} and SIRM); magnetic mineralogy related parameters (Soft and Hard) and magnetic grain size indicators (χ_{ARM}/χ and χ_{ARM}/SIRM) have relatively high values in the upper portions of the cores. The values undergo down-core drop in the middle portions before maintaining an almost constant trend in the bottom portions of the respective cores. So, one can divide the entire core into three sections from the bottom, according to the variations of the magnetic parameters. The mean with standard deviations of all the magnetic parameters for the different sections of the cores are given in Table 3.

1. Section M1 (60–40 cm in core MAA, 76–50 cm in core MR, 66–50 cm in core GH) — This section has low values for all the magnetic parameters studied except for S_{300}. The values of χ, χ_{ARM}, SIRM and $Hard_{IRM}$ have almost constant trends while grain size index ratios fluctuate. S_{300} shows enrichment in the bottom layer of core MAA and core GH while a slight increase towards the surface of this section is noticed in core MR.
2. Section M2 (40–30 cm in core MAA, 50–30 cm in core MR, 50–42 cm in core GH) — In cores MAA and GH, all the parameters undergo a sudden increase especially in the upper 4–6 cm of this section except for χ_{fd} in core MAA and χ_{fd}, χ_{ARM} in core GH which exhibit fluctuations. S_{300} values increase sharply from this depth to the top of this section in both the cores. These changes indicate that the dominant magnetic minerals rapidly change from high-coercivity components to low-coercivity minerals. $Hard_{IRM}$ values too, progressively increase towards the surface indicating that the partial increase of high-coercivity minerals took place in this section. In core MR the trends are slightly different. χ, SIRM, $Hard_{IRM}$ profiles mark this layer with increasing trends towards the surface while χ_{ARM} and granulometric index ratios (χ_{ARM}/χ and χ_{ARM}/SIRM) show remarkable change from 46 to 39 cm depth. S_{300} exhibits a decreasing trend.
3. Section M3 (30–0 cm in cores MAA and MR, and 42–0 cm in core GH) — In this section, all the parameters are found to be enriched in all the cores. S_{300} values suggest that this section is magnetically dominated by low-coercivity ferrimagnetic minerals together with a strong contribution from anti-ferromagnetic minerals. The magnetic granulometric index displays a slight increase in the lower portion of this layer in core MR while in cores MAA and GH an almost constant trend is seen.

3.3.1. Identification of magnetic phase

In cores MAA, MR and GH, sample from sections M2 and M3 show similar curves with the IRM, so only plots of sections M1 and M3 are shown. In Fig. 5, sample from sections M1 and M3 undergo a

Please cite this article as: Singh, K.T., et al., Changing environmental conditions in recent past — Reading through the study of geochemical characteristics, magnetic parameters..., Palaeogeography, Palaeoclimatology, Palaeoecology (2013), http://dx.doi.org/10.1016/j.palaeo.2013.04.008

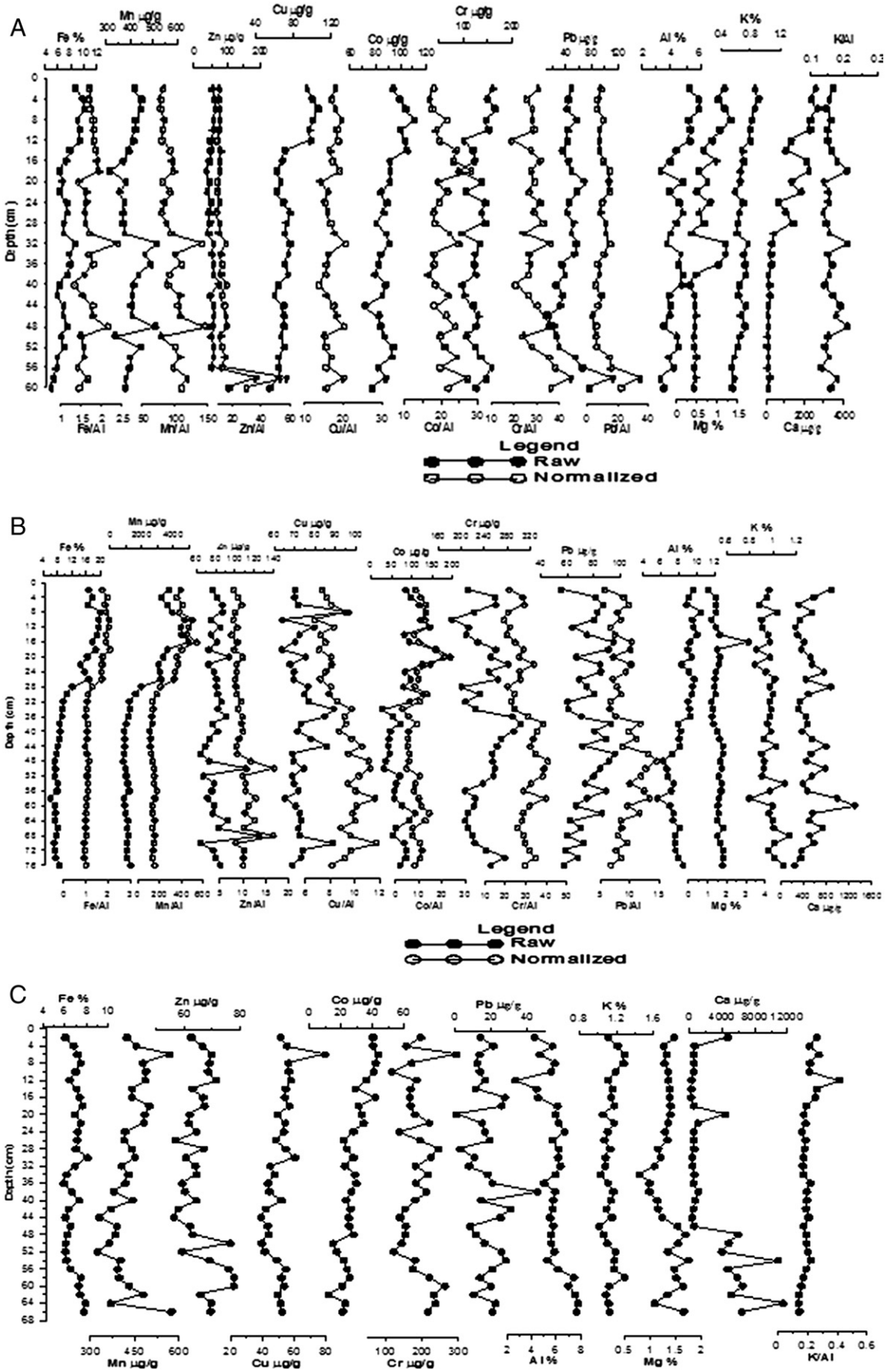

Fig. 3. Down core variation of metals: A — core MAA, B — core MR and C — GH.

Please cite this article as: Singh, K.T., et al., Changing environmental conditions in recent past — Reading through the study of geochemical characteristics, magnetic parameters..., Palaeogeography, Palaeoclimatology, Palaeoecology (2013), http://dx.doi.org/10.1016/j.palaeo.2013.04.008

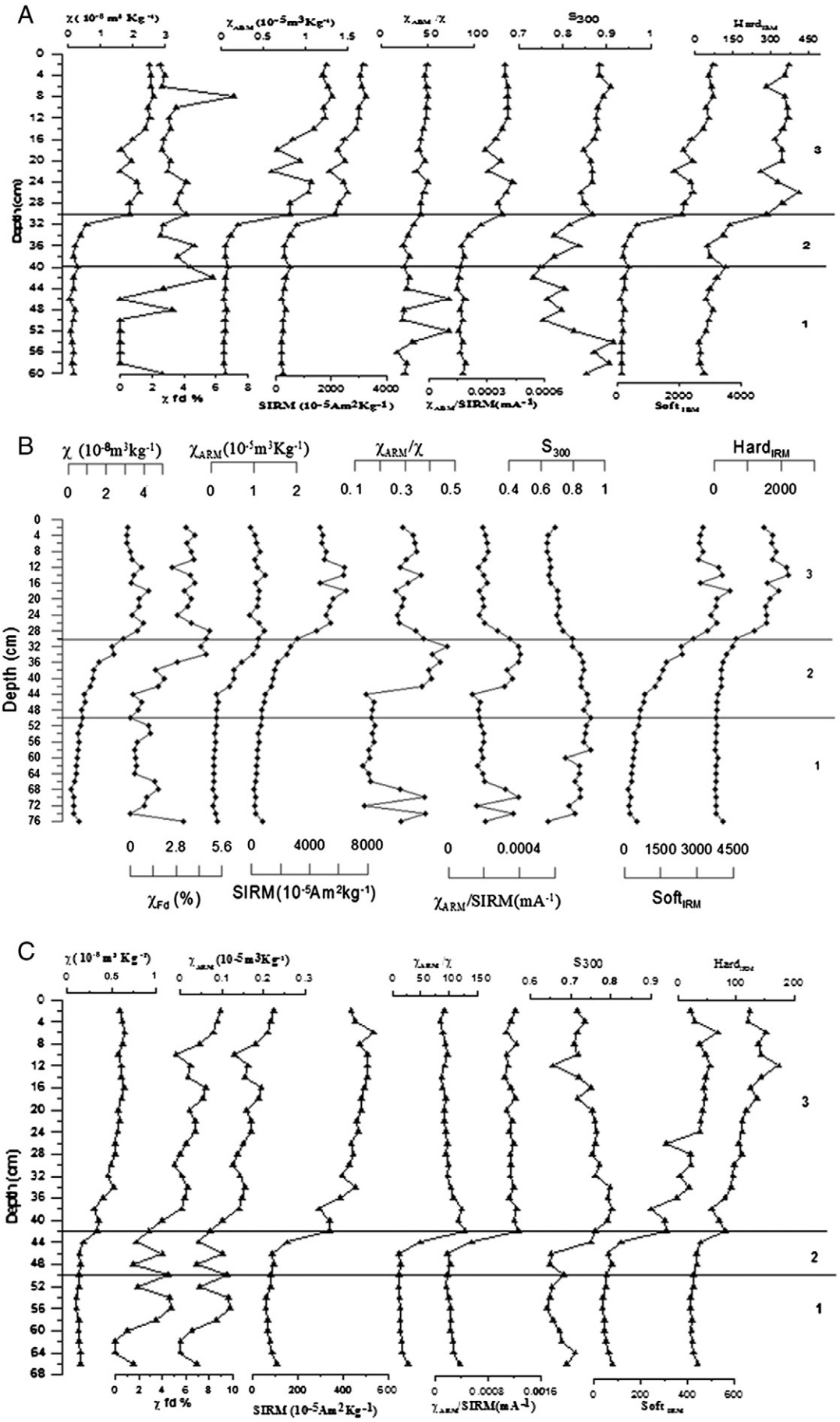

Fig. 4. Magnetic profiles: A — core MAA, B — core MR and C — Core GH.

Please cite this article as: Singh, K.T., et al., Changing environmental conditions in recent past — Reading through the study of geochemical characteristics, magnetic parameters..., Palaeogeography, Palaeoclimatology, Palaeoecology (2013), http://dx.doi.org/10.1016/j.palaeo.2013.04.008

Table 2a
Pearson correlation matrix in core MAA (n = 30).

	Fe	Mn	Zn	Cu	Cr	Co	Pb	K	Mg	Ca	Al	Sand	Silt	Clay	OC
Mn	0.50**	1.00													
Zn	−0.29	0.04	1.00												
Cu	0.93**	0.37*	−0.12	1.00											
Cr	0.39*	0.29	0.24	0.49**	1.00										
Co	0.64**	0.09	−0.09	0.69**	0.22	1.00									
Pb	−0.28	−0.23	0.63**	−0.12	0.30	0.02	1.00								
K	0.92**	0.49**	−0.20	0.86**	0.33	0.52**	−0.32	1.00							
Mg	0.81**	0.43*	−0.14	0.74**	0.48**	0.57**	0.08	0.74**	1.00						
Ca	0.60**	−0.17	−0.25	0.65**	0.31	0.62**	0.08	0.58**	0.62**	1.00					
Al	0.79**	0.25	−0.24	0.83**	0.43*	0.54**	−0.23	0.71**	0.58**	0.53*	1.00				
Sand	−0.43*	−0.50**	−0.07	−0.53**	−0.48**	−0.31	0.22	−0.48**	−0.27	−0.08	−0.46**	1.00			
Silt	0.47**	0.43*	−0.05	0.57**	0.47**	0.44*	−0.25	0.53**	0.31	0.28	0.48**	−0.95**	1.00		
Clay	0.34	0.52**	0.18	0.45**	0.44*	0.16	−0.17	0.39*	0.21	−0.11	0.39*	−0.96**	0.82**	1.00	
OC	−0.50**	0.10	0.54**	−0.37*	0.18	−0.32	0.27	−0.47**	−0.41*	−0.60**	−0.37*	−0.36*	0.20	0.49**	
Mud	0.43*	0.50**	0.07	0.53**	0.48**	0.31	−0.22	0.48**	0.27	0.08	0.46**	−1.00	0.95**	0.96**	1.00

* $p < 0.05$.
** $p < 0.01$.

Table 2b
Pearson correlation matrix in core MR (n = 38).

	Fe	Mn	Zn	Cu	Cr	Co	Pb	K	Mg	Ca	Al	Sand	Silt	Clay	OC
Mn	0.97**	1.00													
Zn	−0.03	−0.03	1.00												
Cu	−0.08	−0.14	0.09	1.00											
Cr	−0.17	−0.25	−0.08	−0.06	1.00										
Co	0.67**	0.65**	0.00	−0.10	−0.15	1.00									
Pb	0.12	0.11	−0.33*	−0.23	0.32	−0.01	1.00								
K	−0.19	−0.20	−0.02	0.03	−0.12	−0.17	−0.03	1.00							
Mg	−0.32	−0.31	0.40**	0.29	−0.20	−0.24	−0.53**	0.05	1.00						
Ca	−0.09	0.05	−0.05	−0.12	0.05	−0.10	0.30	−0.08	0.10	1.00					
Al	0.81**	0.74**	0.03	0.24	−0.18	0.53**	−0.17	−0.22	−0.02	−0.23	1.00				
Sand	−0.61**	−0.62**	−0.06	−0.18	0.34*	−0.46**	−0.04	0.21	0.13	−0.03	−0.57**	1.00			
Silt	0.46**	0.39*	−0.06	0.34*	−0.02	0.32	0.13	−0.12	−0.40**	−0.30	0.64**	−0.57**	1.00		
Clay	−0.21	−0.13	0.10	−0.30	−0.17	−0.13	−0.12	0.03	0.40**	0.37*	−0.45**	0.11	−0.88**	1.00	
OC	−0.91**	−0.86**	0.06	0.04	0.13	−0.59**	−0.07	0.10	0.37	0.21	−0.83**	0.51**	−0.61**	0.45**	
Mud	0.60**	0.61**	0.05	0.18	−0.34	0.44**	0.05	−0.21	−0.13	0.03	0.56**	−1.00	0.56**	−0.11	1.00

* $p < 0.05$.
** $p < 0.01$.

monotonous decay until their unblocking at ~680 °C. The most distinct difference for samples from section M1, compared to those from higher parts of all the cores is that there is considerable decrease from 150 to 350 °C. Gregite has higher coercivity than magnetite (Roberts, 1995) and is characterized by loss of most of its magnetization from 200 °C to 350 °C (Reynolds et al., 1994; Roberts, 1995; Torii et al., 1996). In contrast, pyrrhotite undergoes rapid unblocking within a much narrower temperature range of 320–350 °C (Dekkers, 1989; Torii et al., 1996). There is possibility that the loss in magnetization at around 200–320 °C is due to maghemite or titanomagnetite. Finally, the values are unblocking to near zero at about 580 °C, which suggests that magnetite is also the dominant one in this section.

Table 2c
Pearson correlation matrix in core GH (n = 33).

	Fe	Mn	Zn	Cu	Cr	Co	Pb	K	Mg	Ca	Al	Sand	Silt	Clay	OC
Mn	0.53**	1.00													
Zn	0.24	0.23	1.00												
Cu	0.55**	0.75**	0.36*	1.00											
Cr	0.44**	0.42*	0.28	0.52**	1.00										
Co	0.08	0.46**	−0.04	0.57**	−0.03	1.00									
Pb	−0.21	−0.33	−0.12	−0.24	−0.15	−0.07	1.00								
K	0.02	−0.18	0.44**	−0.15	0.21	−0.43**	0.08	1.00							
Mg	0.22	0.23	0.39*	0.50**	0.12	0.37*	0.21	0.02	1.00						
Ca	0.02	0.12	0.43**	0.06	−0.10	−0.10	−0.14	0.49**	0.12	1.00					
Al	0.50**	−0.04	0.19	−0.15	0.26	−0.53**	−0.05	0.43**	−0.01	0.01	1.00				
Sand	−0.28	−0.46**	−0.62**	−0.56**	−0.25	−0.44**	0.06	−0.24	−0.51**	−0.39*	0.01	1.00			
Silt	−0.23	−0.38*	0.11	−0.25	−0.02	−0.28	0.05	0.41*	0.18	0.24	0.22	−0.02	1.00		
Clay	0.36*	0.58**	0.25	0.53**	0.16	0.48**	−0.07	−0.21	0.14	−0.01	−0.19	−0.54**	−0.83**		
OC	−0.43**	−0.58**	−0.11	−0.69**	−0.13	−0.62**	0.23	0.25	−0.40*	0.07	0.16	0.50**	0.53**	−0.73**	
Mud	0.29	0.46**	0.61**	0.56**	0.26	0.43**	−0.04	0.25	0.53**	0.35	−0.01	−0.99**	0.01	0.55**	1.00

* $p < 0.05$.
** $p < 0.01$.

Please cite this article as: Singh, K.T., et al., Changing environmental conditions in recent past — Reading through the study of geochemical characteristics, magnetic parameters..., Palaeogeography, Palaeoclimatology, Palaeoecology (2013), http://dx.doi.org/10.1016/j.palaeo.2013.04.008

Table 3
Mean concentration with the standard deviation of magnetic parameters in the different cores studied.

		Core MAA	Core MR	Core GH
$\chi \times 10^{-8} m^3\ kg^{-1}$	Section M3	2.201 ± 0.354	3.493 ± 0.381	0.532 ± 0.105
	Section M2	0.322 ± 0.160	1.329 ± 0.613	0.149 ± 0.022
	Section M1	0.135 ± 0.054	0.423 ± 0.141	0.125 ± 0.016
$\chi_{ARM} \times 10^{-5} m^3\ kg^{-1}$	Section M3	1.02 ± 0.23	1.08 ± 0.10	0.51 ± 0.06
	Section M2	0.10 ± 0.06	0.48 ± 0.36	0.04 ± 0.03
	Section M1	0.04 ± 0.08	0.08 ± 0.03	0.02 ± 0.01
$SIRM \times 10^{-5} A\ m^2\ kg^{-1}$	Section M3	2671 ± 421	5193 ± 850	445 ± 62
	Section M2	457 ± 189	1453 ± 704	105 ± 33
	Section M1	238 ± 60	391 ± 164	76 ± 16
S_{300}	Section M3	0.87 ± 0.02	0.69 ± 0.04	0.75 ± 0.04
	Section M2	0.79 ± 0.03	0.86 ± 0.03	0.68 ± 0.05
	Section M1	0.82 ± 0.06	0.82 ± 0.07	0.67 ± 0.02
$Soft_{IRM} \times 10^{-3} A\ m^{-1}$	Section M3	2575 ± 416	3502 ± 438	414 ± 74
	Section M2	371 ± 176	1371 ± 659	76 ± 26
	Section M1	172 ± 47	344 ± 125	51 ± 15
$Hard_{IRM} \times 10^{-3} A\ m^{-1}$	Section M3	339 ± 39	1643 ± 379	114 ± 28
	Section M2	95 ± 40	216 ± 151	32 ± 5
	Section M1	44 ± 23	72 ± 61	25 ± 4
χ_{fd} (%)	Section M3	3.45 ± 1.14	3.67 ± 0.57	6.32 ± 1.46
	Section M2	3.56 ± 0.93	1.84 ± 1.65	2.95 ± 1.52
	Section M1	1.44 ± 2.04	0.93 ± 0.87	2.46 ± 1.82
χ_{ARM}/χ	Section M3	0.5 ± 0.04	0.3 ± 0.04	10 ± 1.0
	Section M2	0.3 ± 0.04	0.3 ± 0.1	0.2 ± 0.1
	Section M1	0.4 ± 0.2	0.2 ± 0.1	0.2 ± 0.1
$\chi_{ARM}/SIRM\ (m\ A^{-1})$	Section M3	0.0004	0.0002	0.0012
	Section M2	0.0002	0.0003	0.0003
	Section M1	0.00016	0.0002	0.0003

χ (T) curves for heating–cooling cycles from room temperature up to 700 °C from core MAA, core MR and core GH from section M1 are presented in Fig. 5B. For the sample from section M1, χ is low even to negative values in between and fluctuating from room temperature to 300 °C, which suggests a dominant contribution from paramagnetic minerals. The decrease in χ up to ~300 °C is followed by an increase in χ from 300 to 350 °C and a marked increase in χ from 350 to 460 °C. The increase in χ at ~300 °C could be due to the presence of gregite, and might signal the onset of thermal alteration of gregite into magnetite or maghemite (Dekkers et al., 2000). Upon cooling a marked increase in χ occurs between ~580 and 450 °C, which indicates the production of a significant amount of magnetite during heating. So, it can be concluded that in all the cores, the magnetic properties of section M3 and M2 contain substantial contributions from hematite as well as magnetite. In contrast, the magnetic mineralogy of section M1 is characterized by (titano)magnetite and gregite, with little hematite.

The results of concentration dependent magnetic parameters (χ, χ_{ARM} and SIRM) indicate the presence of ferrimagnetic minerals in all the three cores. The high values of magnetic mineralogy related parameters (S_{300}, $Soft_{IRM}$ and $Hard_{IRM}$) indicate the presence of magnetite. Among the magnetic grain size indicators (χ_{fd} %, χ_{ARM}/χ and $\chi_{ARM}/SIRM$), χ_{ARM}/χ is sensitive to the crystalline grain size of ferrimagnetic minerals. Higher χ_{ARM}/χ values reflect more Stable Single Domain (SSD) grains and lower values reflect more Multi-Domain (MD) or Super-Paramagnetic (SP) grains. The results show that the magnetic grain size indicators in the sediment cores are dominated by fine grained SSD ferrimagnetic minerals. It is seen that the concentration dependent magnetic parameters, magnetic mineralogy related parameters and magnetic grain size indicators have relatively high values in the upper portions of all the cores (section M3), with nearly constant values of S_{300} and granulometric index in all the cores. The section M3 is therefore interpreted to be the least affected by early diagenetic influence. The main magnetic minerals in this part of the cores (magnetite and hematite) can be regarded as the primary detrital magnetic minerals prior to diagenetic modifications in the underlying section. The initial diagenetic stage, observed in section M2 begins with sharp decrease in ferrimagnetic mineral concentration. The concentrations decline progressively with depth with absolute minimum abundance being attained at the upper end of this section. This stage is associated with depletion of the high-coercivity components. The late diagenetic stage, as observed in section M1 (Fig. 4), is characterized by authigenic production of fine-grained ferrimagnetic minerals. Similar observations are reported by Venkatachalapathy et al. (2011).

3.4. ^{210}Pb dating

In cores MAA, MR and GH, there is a relatively log-linear decrease of $^{210}Pb_{excess}$ activity with depth (Fig. 6) but with a change in slope at 10 cm in core MAA, 36 cm in core MR and 26 cm in core GH. Changing slope in the $^{210}Pb_{excess}$ profile indicates variation in accumulation rate which may be due to bioturbation (Cundy and Croudace, 1995). The assumption of a closed system might be violated in salt marshes due to early diagenetic remobilization of ^{210}Pb (Allen et al., 1993; Cundy, 1994). If no diagenetic remobilization occurs then the annual flux will be relatively constant (Crozaz et al., 1964). When the profiles of $^{210}Pb_{excess}$ are compared with Pb and redox sensitive elements, no similar peaks are observed, negating the possibilities of mobilization of ^{210}Pb. The higher values of $^{210}Pb_{excess}$ at the top 10 cm in core MAA, 36 cm in core MR and 26 cm in core GH do not coincide with the proposed oxidized/partially reducing boundary and not even with partially reducing/reducing boundary. However, the $^{210}Pb_{excess}$ concentration minima for cores MAA, MR and GH occur below 35, 45 and 42 cm onwards, which if taken as background values, may highlight the possibility of diagenetic movement, as 30 cm for core MAA, 38 cm for core MR and 32 cm for core GH were the transition in colors recorded in the field. Hence, in the present study, there is no obvious change in the shape of $^{210}Pb_{excess}$ profiles in the vicinity of the proposed oxidized/reduced as would be expected if ^{210}Pb migration had taken place. Therefore, the change in slope strongly suggests a change in sedimentation pattern. In core MAA, the sedimentation was slower at 0.31 cm/yr until 10 cm, which corresponds to the year 1996 and increased thereafter to 1.21 cm/yr; in core MR it was slower at 0.14 cm/yr until 35 cm, which corresponds to year

Please cite this article as: Singh, K.T., et al., Changing environmental conditions in recent past — Reading through the study of geochemical characteristics, magnetic parameters..., Palaeogeography, Palaeoclimatology, Palaeoecology (2013), http://dx.doi.org/10.1016/j.palaeo.2013.04.008

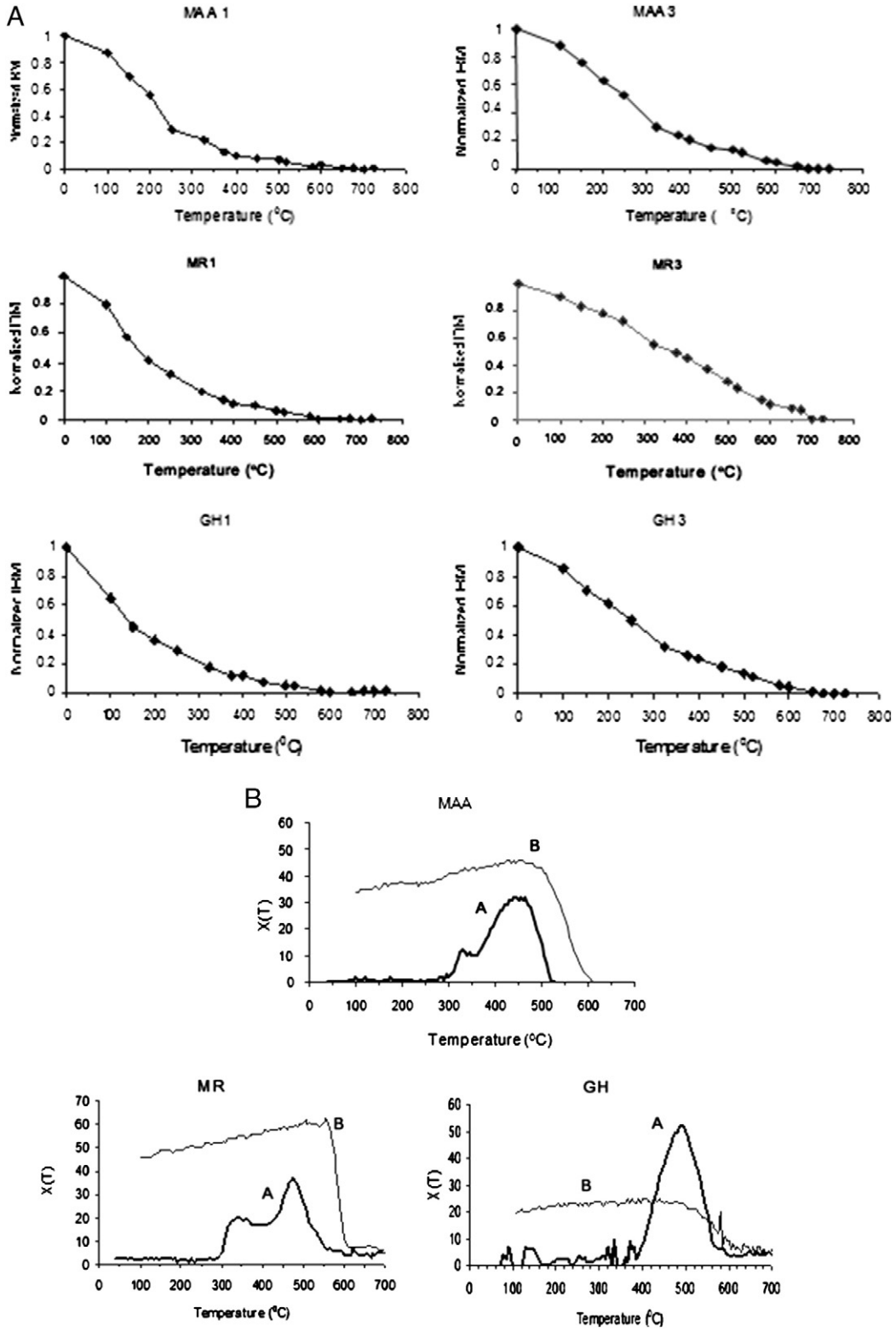

Fig. 5. A. Representative thermal demagnetization curves for different sections in core MAA, core MR and core GH. B. Representative curve of temperature dependence of magnetic susceptibility (A — Heating, B — Cooling).

~1980 and increased thereafter to 1.42 cm/yr while in core GH the sedimentation rate was slower at 0.16 cm/yr until 26 cm, which corresponds to the year 1992 and increased thereafter to 2 cm/yr which may be due to catchment area geology and processes both natural and anthropogenic. Based on this observation, the bottom of cores MAA, MR and GH date back to 1835, 1694 and 1732 years, respectively.

4. Discussion

4.1. Statistical analysis

4.1.1. Correlation analysis

In order to understand the relationship between the metals and sediment components, Pearson's correlation tests were carried out

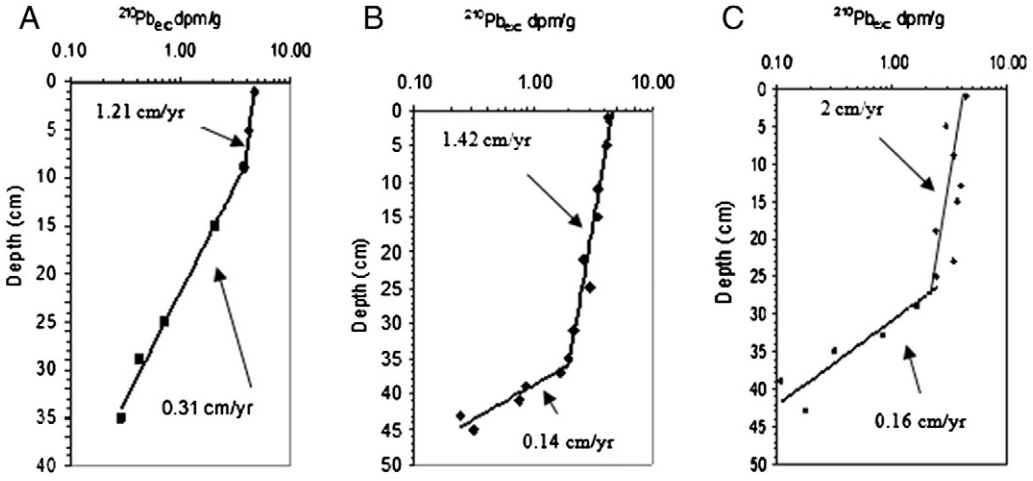

Fig. 6. Down core profiles of ^{210}Pb: A — core MAA, B — core MR and C — core GH.

for the data set of each core. The correlation matrices for the three cores are shown in Tables 2a, 2b and 2c. In core MAA, Al shows good correlations with sediment components (silt, clay) and metals such as Fe, Co, Cu and Cr, which indicates the association of metals with finer fraction of sediments and detrital source. Therefore, the metals are normalized to Al. Fe shows good correlations with almost all the elements as compared to Mn, signifying the role of Fe in redistribution of the metals. However, the strong correlation of Al with Fe and subsequently with Cu, Co and Cr points to their common origin rather than diagenetic precipitation. In core MR, the profiles of Mg, K and Ca (Fig. 3B) do not bear any similarities with the sediment component profiles and also with heavy metals including Fe and Mn. On the other hand, the correlations between the mud content and Al in the sediments are statistically significant (Table 2b) which indicate that Al must be dominantly present in the finer fraction so the use of Al concentration as a proxy for finer fraction of sediment is valid in this core. Al shows significant correlations with Fe, Mn and Co but very poor correlations with the remaining elements suggesting a different, possibly an anthropogenic source. Fe and Mn show significant enrichments in the upper portion of the core but without any coincident peaks between them and the other metals. This observation along with the non-supportive nature of Ca negates the possibility of post depositional movements in this core. Hence the enrichment of Fe and Mn in the upper portion of the core may have an anthropogenic origin rather than an early diagenetic origin.

In core GH, the profiles of the major elements do not agree with any of the sediment component profiles. Heavy metals also show poor associations with Al and clay indicating that clay does not play a role in metal absorption. The profiles are, therefore, presented in raw (Fig. 3C), rather than being normalized as suggested by Ackermann (1980) and Grant and Middleton (1990). However, the distribution profiles may be partially due to early diagenesis processes (Berner, 1980) as well as environmental contamination (Anderton, 1985). Mn shows significant correlations with Cu, Cr and Co while Fe maintains an association with only Cu and Cr. Mn to some extent is found to exhibit better correlations than Fe, signifying its role in redistribution of the heavy metals. The good associations of Co with Mn than Fe reflect recycling of Co along with Mn oxides at redox boundaries (Zwolsman et al., 1993). The exclusive role played by Mn oxides in the cycling of Ni and Co has been reported earlier by Klinkhammer (1980) and Shaw et al. (1990). The reason for the evidence of digenetic modifications can be seen with the peaks of Zn, Cu, Cr and Co at 6 cm depth which coincides with Mn peak and also peaks of Zn, Cu (28 and 40 cm) and Cr (28 cm) with Fe and Mn peaks, which indicate their coprecipitation with Fe and Mn oxides.

4.1.2. Principal component analysis (PCA)

PCA was applied to the dataset to judge the sources of sediments and distinguish the natural and anthropogenic inputs in the three cores. This method of analysis has been used by other researchers

Table 4
Varimax normalized factor analysis: A — core MAA, B — core MR and C — core GH.

Total variance (%)	Core MAA			Core MR			Core GH		
	Factor 1	Factor 2	Factor 3	Factor 1	Factor 2	Factor 3	Factor 1	Factor 2	Factor 3
	44.88	21.07	12.72	35.51	14.93	13.42	33.03	19.28	12.06
Fe	**0.87**	0.34	−0.23	**−0.96**	0.08	−0.07	−0.26	0.09	**0.81**
Mn	0.16	0.66	−0.12	**−0.96**	0.06	0.05	−0.66	0.14	0.49
Zn	−0.22	0.12	**0.81**	0.00	−0.58	−0.03	−0.07	**0.76**	0.28
Cu	**0.87**	0.39	−0.03	0.12	−0.36	−0.61	**−0.73**	0.31	0.40
Cr	0.43	0.43	0.53	0.31	0.52	−0.10	−0.09	0.16	0.69
Co	**0.75**	0.12	0.07	**−0.75**	0.01	−0.01	**−0.84**	0.07	−0.24
Pb	0.03	−0.30	**0.90**	−0.06	**0.80**	0.17	0.13	0.06	−0.39
K	**0.79**	0.39	−0.25	0.26	−0.05	−0.38	−0.38	0.60	−0.06
Mg	**0.84**	0.17	0.07	0.27	**−0.81**	0.11	0.11	0.68	−0.04
Ca	**0.87**	−0.19	0.04	0.00	0.12	0.51	0.51	0.62	0.21
Al	**0.75**	0.35	−0.15	**−0.79**	−0.17	−0.44	0.50	0.11	0.67
Sand	−0.20	**−0.94**	−0.05	**0.72**	0.13	0.15	0.49	**−0.74**	−0.15
Silt	0.32	**0.84**	−0.01	−0.46	0.23	**−0.79**	0.62	0.47	−0.21
Clay	0.06	**0.96**	0.11	0.15	−0.34	**0.87**	**−0.79**	0.01	0.26
OC	−0.64	0.49	0.49	**0.87**	−0.14	0.30	**0.84**	−0.07	−0.24

The bold values represent significant positive/negative correlation among the variables in each factor.

(Fernandes et al., 2011; Wang et al., 2011) on environmental data. The results of the analysis with varimax rotation are shown in Table 4. In core MAA, three factors representing 78.68% of the total variance are identified. Factor 1 accounts for 44.88% of the total variance and is characterized by high positive loadings (>0.5) on Fe, Cu, Co, K, Mg, Ca and Al. This factor represents the association of metals with major elements which probably indicates the detrital origin of both marine and terrigenous sources. Factor 2 accounts for 21.07% of the total variance and is characterized by high positive loadings on silt, clay and OC and strong negative loadings on sand suggesting association of organic carbon with finer detrital components of sediments. Within this factor, two mutually exclusive groups of metals are distinguished, associated with clay and silt (Fe, Mn, Cu, Cr, K and Al) and with sand (Ca and Pb). Factor 3 accounts for 12.72% of the total variance and is characterized by high positive loadings on Zn, Cr and Pb and negative loadings on Al, K and silt that may suggests an anthropogenic origin.

In core MR, three factors representing 63.86% of total variance are identified (Table 4). Factor 1 accounts for 35.51% of the total variance and is characterized by high positive loadings (>0.5) on sand, organic carbon and negative loadings on Fe, Mn, Co, Al and silt indicating the strong association of metals with finer fraction of sediments. This group of elements does not correlate with the other major elements such as Mg and K, which probably reflects the anthropogenic signals that masked the contribution made by detrital components. Factor 2 accounts for 14.93% of the total variance and is dominated by the high positive loadings on Pb, Cr and negative loading on Zn and Mg, thus reflecting the different source of Cr, Pb and Zn probably from industrial and urban sources. Factor 3 accounts for 13.42% of the total variance and is dominated by the high positive loadings on Ca, clay and negative loading on Cu and silt, thus reflecting the detrital source controlled by the silt and clay components. The opposite relationship between clay and silt within this group allows distinguishing of two mutually exclusive groups, as there is a factor of physical control that selects the sediment according to its size.

In core GH, three factors representing 64.38% of the total variance are identified. Factor 1 accounts for 33.03% of the total variance and is characterized by high positive loadings (>0.5) on Al, Ca, sand, silt and organic carbon and high negative loadings on Fe, Mn, Cu, Co and clay. This factor represents the association of metals with finer fraction indicating that the environmental dynamic conditions exert control over them and probably are of detrital origin. Factor 2 accounts for 19.28% of the total variance and is characterized by high positive loadings on Zn, K, Mg, Ca and silt and negative loadings on sand and OC. This may suggest the strong association of metals with silt probably of marine origin. Factor 3 accounts for 12.06% of the total variance and is characterized by high positive loadings on Fe, Mn, Cu, Cr and Al. This factor is similar to factor 1.

The PCA analysis indicated the role of grain size and Fe–Mn oxides in the distribution of metals in the different cores studied.

In all the three cores studied, in the upper 20 cm, sand decreases and clay increases towards the surface. With respect to OC, high amounts of OC are seen at the bottom of core MAA while the other two cores do not show such an observation. This may be probably governed by factors such as source, sedimentation and post depositional processes in addition to the grain size parameters and energy conditions. Kumaran et al. (2004) have reported lignite beds exposed in Kolamb well-section near Malvan area and have further cited that these lignites are autochthonous and deposited in near-shore environment. Therefore, the high percentage of OC in this particular core can be related to the lignite source which must have been deposited in calm energy and preserved under reducing conditions. When the metal distribution is seen in the three cores, core MR is found to be significantly enriched with almost all the trace metals as compared to the metal concentrations in sediments from core MAA and core GH. The spatial distributions of the measured trace metal concentrations strongly suggest that the main sources of the contamination in core MR are land based. When the down core profiles are observed, higher metal contents and clay component are observed in the uppermost sediment layers, while values are generally relatively low and stable in the deeper layers, which might represent the natural background signatures or a fairly clean natural environment with little pollution. The vertical profiles of the three cores show an increase in the metal concentrations especially in core MR, suggesting that contamination rates continue to increase to the present day. High magnetic susceptibility values are also observed in the upper portions (section M3) of all the three sediment cores and could result from different mechanisms, such as diagenetic changes in magnetic mineralogy (Karlin et al., 1987), an increased input of detrital magnetite from soil erosion (Maher and Taylor, 1988; Higgitt et al., 1991) or a greater magnetotactic bacteria concentration in the surface sediment (Lovley et al., 1987). In this study, significant enhancement of magnetic concentration dependent parameter values in the uppermost section, followed by rapid decrease with depth indicate the presence of fine grained ferrimagnetic (Fe oxides) minerals in the upper portion of the cores which might be derived from anthropogenic activities (Chan et al., 1998, 2001).

4.2. Associations between metals and magnetic parameters

The relationships between heavy metals and magnetic parameters have provided interesting information on heavy metal sources and pathways. It has been demonstrated that environmental magnetism can be used as a proxy indicator of heavy metal concentration in a simple, quick and non-destructive way (Goddu et al., 2004; Lu and Bai, 2006). The magnetic parameters are extremely sensitive and small changes in catchment area processes would be recorded in the sediments. Therefore one can hypothesize some relationship between geochemical indicators of erosion, i.e. Al, Mg, K and Na (Mackereth, 1966) and the dominant remanence carriers of the magnetic signal (e.g. SIRM). The good relationship (Pearson's correlation) between the SIRM with Al ($p < 0.01$, $r = 0.59$), K ($p < 0.01$, $r = 0.55$) and Mg ($p < 0.01$, $r = 0.56$) in core MAA suggests the catchment area processes as one of the explanations for the variations in magnetic properties with depth. However, no significant relationships of SIRM with Mg and K in core MR and of SIRM with Al, Mg and K in core GH are seen indicating little supporting evidence of catchment changes (Mackereth, 1966).

In core MAA, χ and χ_{ARM} show poor correlations with clay but they show good correlations ($p < 0.01$, $r < 0.60$) with Fe, Cu and Co. On the other hand in core GH, χ_{ARM} shows good correlation ($p < 0.01$, $r < 0.50$) with clay, but poor correlations with the metals studied except Co. Considerable similarity between the heavy metals and χ_{ARM} was reported from intertidal sediments of the Yangtze Estuary, China by Zhang et al. (2001). Zhang et al. (2007) reported the strong relationship between χ_{ARM} and to a lesser degree, χ_{fd} with heavy metals and explained the role of particle size effects and Fe oxides in controlling metal concentration. In the present study, χ_{ARM} in core MR shows good correlations with mud ($p < 0.01$, $r = 0.60$) and Al ($p < 0.01$, $r = 0.80$) which indicates that there is close association between fine grained fraction and fine grained magnetite. There are also significant correlations between magnetic properties (χ, χ_{ARM} and SIRM) and metals such as Fe, Mn and Co. Most important, there is similarity in trends of $Hard_{IRM}$ and $Soft_{IRM}$ profiles with metals, which points to a possible common anthropogenic nature of the magnetic mineral carrier. So, the close correlation of the different magnetic profiles with the variations in heavy metal concentrations including Fe and Mn strongly reflect trace metal enrichment in recent years with magnetically enhanced soil derived clays during weathering and transportation.

In core MR, the mean values of χ, ARM and SIRM in section M3 are several fold higher than those of section M1 (Table 3). The strong

Please cite this article as: Singh, K.T., et al., Changing environmental conditions in recent past — Reading through the study of geochemical characteristics, magnetic parameters..., Palaeogeography, Palaeoclimatology, Palaeoecology (2013), http://dx.doi.org/10.1016/j.palaeo.2013.04.008

magnetization suggests that there is a much greater magnetic input to the upper sediment layers. Mining in Goa contributes to about 10% of the total economy (Sardesai, 1985) with iron ore being the most predominant in terms of both production and export. Regular export of iron ore in Goa started only in the year 1947 and most of the iron ore was exported to Japan. The mines were principally active from 1905 and there were only few refineries characterized by low-volume operations and low stacks. Actual mining in Goa started from 1949 to 1950. For the first ten years it was manual and the production was mainly manganese and ferromanganese. During 1971–1980, Goa accounted for 32% of the country's total iron ore production and 55% of its export (Swaminathan, 1982). Since the 1980s, industrialization and urbanization around the Goa region has accelerated resulting in increase of pollution around the estuarine areas. This is reflected well by the elevated contents of heavy metals and magnetic minerals seen in the sediment profile (35 cm and above). These parameters have been increasing continuously since then and peaked in the 1990s (20 cm), and have remained at a high level since then (Figs. 3B and 4B). From 1990 onwards, the exports from Goa accounted for over 40%. The enrichment of Fe and Mn in the upper portion of the core along with the profiles of most of the trace metals increased rapidly after 1980. Based on these observations, the environmental history of the Goa region can be divided into pre-1980 period, during which the anthropogenic impacts were less and post-1980 period, during which the anthropogenic impacts became dominant.

Changes in magnetic properties under conditions of varying temperatures or magnetic fields provide information on type of minerals present and on their particle size (Deng et al., 2000; Laj et al., 2000). Thermomagnetic and temperature measurements suggest the presence of gregite in section M1. Sedimentary gregite has been consistently found to have Single Domain (SD) like magnetic properties (Snowball, 1991; Roberts, 1995). The higher OC content in section M1 for all the three cores could have contributed to gregite preservation through a mechanism suggested by Kao et al. (2004). Fine grained gregite bearing sediments from Southwestern Taiwan had high OC contents at high Fe activity compared to sediments not containing gregite. Kao et al. (2004) argued that high Fe activity might have suppressed sulfate reduction and removed reduced sulfur so effectively that pyritization was arrested or retarded which would have focused the preservation of intermediate gregite. However, in the present study, the sudden increase in OC and ferrimagnetic minerals together with high sand content may suggest the possibility of more terrigenous input during this time before it was subjected to diagenetic modifications in the later stage. This observation is also reflected through the two phases of sedimentations seen in the three cores. In these cores, sedimentation rates are initially extremely low and then increase >10 fold in Mandovi and Tadri, and by ~4 fold in Kolamb Creek in recent times. The higher rate of sedimentation in all these areas are recorded since 1992 (Gokarn), 1980 (Mandovi) and more recently 1996 (Malvan).

4.3. Probable factors for change in sedimentation rates

Nigam et al. (1995) have reported the variation in paleomonsoons in a cyclic manner of around 77 years by studying a sediment core collected off Karwar on the western continental shelf of India. They have also observed that the period around 1935 was dry showing deficient rainfall while the period around 1984 was wet with high rainfall. Thus, the runoff from rivers due to enhanced monsoonal precipitation over catchment area may facilitate the high rate of sedimentation. The rainfall data of the past 100 years (1901–2005) of Goa also supports the above explained phenomenon. It is observed (Fig. 7) that the annual rainfall started increasing from around 1955, then was uniformly high around the 1980s again gradually increased until 2000 and then it started decreasing. This is supported by the higher clay percentage observed between 1988 and 2000 in core

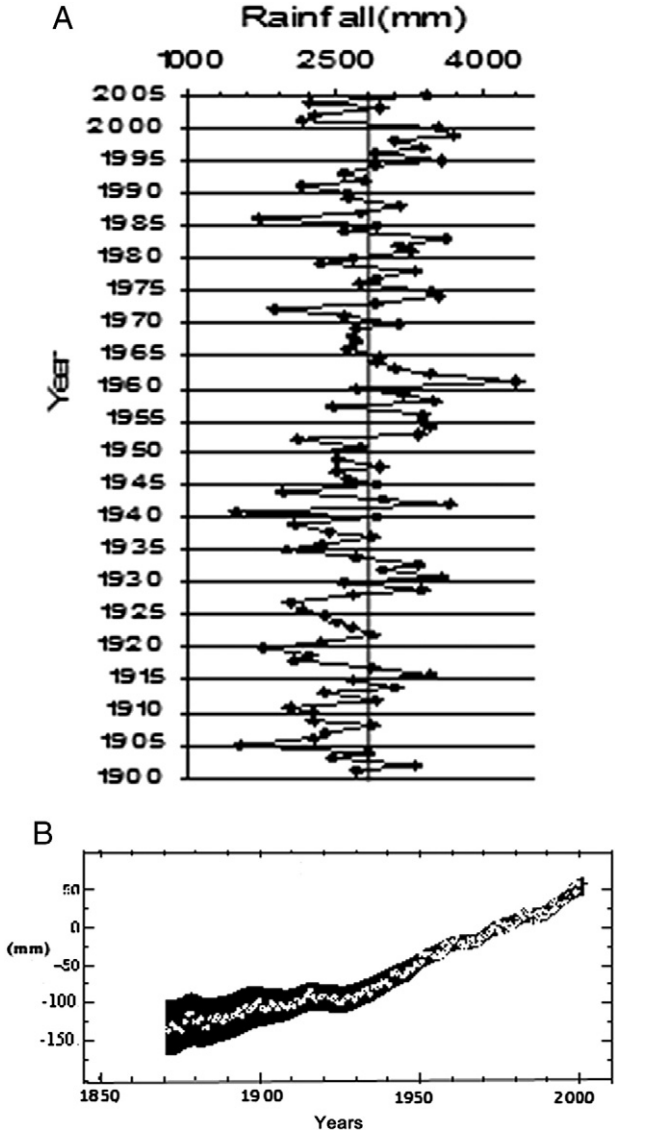

Fig. 7. A. Variation of annual rainfall in Goa during the last 100 years. B. Global average sea level rise (after 4 reports, IPCC, 2007).

MR. Also, in this core one can see well preserved χ, Fe and Mn profiles, wherein a sudden increase in value is seen from ~36 cm (corresponds to 1980) till the surface of the core (corresponds to 2005).

χ_{fd} consists of very fine grained magnetic crystals (0.03 μm) derived almost exclusively from the weathered part of the soil (Thompson and Oldfield, 1986). These fine crystals are poorly represented both in anthropogenic particles generated by fossil fuel combustion and other industrial activities and in common geological parent materials. In the present study, the enrichment of $\chi_{fd\%}$, Fe and Mn value in the top 36 cm may suggest the higher input of finer materials by the weathering of soils degraded by the mining activities, input of clayey mining rejects, pumped out muddy waters from mines, and slime from beneficiation and pelletization plant (Nayak, 1998). In the 1980s and 1990s, mining became a highly sophisticated, capital intensive industry wherein the annual production of iron ore in Goa was around 15 million tonnes (Nayak, 2002). In 1996–1997, the total mineral ore produced in Goa was 137.37 lakh tonnes of which iron ore consisted of 136.42 lakh tonnes. The iron ore deposits of Goa are essentially of hematite and are associated with ferrogenous quartzite and phylites. Normally, the iron ore mined in the hinterland is transported by trucks to

Please cite this article as: Singh, K.T., et al., Changing environmental conditions in recent past — Reading through the study of geochemical characteristics, magnetic parameters..., Palaeogeography, Palaeoclimatology, Palaeoecology (2013), http://dx.doi.org/10.1016/j.palaeo.2013.04.008

the riverbanks in the upstream region, where it is stored for loading onto barges. During the monsoon, the ore stacked at the river banks gets washed away with rain and the washings drain into the river, carrying along with it the sediments in suspension (Singh et al., 2012). The magnitude of impact of mining is also evident by the distribution of enriched sedimentary metals (Fig. 3B). Higher concentrations of Fe, Mn and Cr in sediments of Mandovi estuary were related to release of mine wastes by Bukhari (1994). The significant increase in metal enrichments starts in the middle of the 1950s, which is in agreement with the later development of mining activities existing along the Mandovi estuarine region, together with the increase of domestic effluents associated with the population growth around the region.

Another factor, besides river discharge, that could be responsible for variations in the sedimentation rate is the local sea level rise, which is directly related to the morphology and sedimentation pattern of the estuary/creeks. According to fourth assessment report of the Inter Governmental Panel on Climate Change (IPCC, 2007), global average sea level rose at an average rate of 1.8 (1.3 to 2.3) mm per year from 1961 to 2003 (Fig. 7B). The rate was faster from 1993 to 2003, i.e. about 3.1 (2.4 to 3.8) mm per year. The average sea level rise for India has been reported as 2.5 mm/year since the 1950s (Das and Radhakrishna, 1993). Agarwal (1990) considered the west coast of India to be an emergent type and identified a rise in sea level to the order of 0.3 m during the past 57 years. Being the largest in this region, Mandovi estuary would be most affected by the sea level rise. Therefore, the rise in sea level may have provided more accommodation for the deposition of the increased amount of sediments released through mining activities in the hinterland. Similarly, in the Tadri creek (core GH), the comparatively wide mouth, next to the Mandovi river, must have resulted in favorable conditions for higher sedimentation rate coupled with availability of the sediments due to sand and lime mining activities in and around the creek. This observation agrees with the link seen between magnetic properties (χ, χ_{ARM} and SIRM) and metals (Pb and Co) in core MAA and between magnetic properties (χ, χ_{ARM} and SIRM) and metals (Mn, Zn and Cu) in core GH in the upper portions of the cores, wherein the rate of sedimentation recorded is very high further suggesting of an anthropogenic source. The χ_{fd} values are found to increase gradually towards the surface along with the metals which may be because of a relatively higher degree of weathering and erosion. This may reflect trace metal enrichment of the magnetically enhanced soil derived clays during weathering and transportation from 1990 onwards with enhanced sedimentation rate. A study carried out along the Ratnagiri coast (close to Malvan) revealed that there was a decreasing trend in the number of macroalgal species within a period of 19 years from 1979 to 1998 (Untawala et al., 1979; Agadi, 1986). They reported that the increase in sedimentation was adversely influencing the algal growth. There are no large scale industries around the Malvan coast. However, mining-related industries have been set up in recent years. At present this industrial activity has little impact on the coastal and marine biodiversity of Malvan coast. In Gokarn also, no large scale industries are present.

In all the three cores, it is observed that finer sediment (mud) was deposited during the higher rate of sedimentation. The increase in finer sediments may reflect the periods of wet and cold climates (Alin and Cohen, 2003). Therefore, the increase of finer sediments from 1980 till the present may be possibly because of the role played by the climate change especially the rainfall. With growing human activities like agriculture, mining, construction and development in the catchment area, in these recent years, there has been alteration of land use patterns. This must have enhanced sediment yields of rivers coupled with higher rainfall resulting in the observed higher rate of sedimentation in the estuarine and creek regions. Similar observations have been reported in other studies (Chan et al., 2001; Syvitski et al., 2005). The distribution of metals and magnetic parameters in the sediment columns thus reflect recent episodes of metal contamination.

5. Conclusion

A study carried out on mudflat sediment cores along the west coast of India using multi-proxy parameters such as sedimentological, chemical, magnetic and also radionuclide, showed depth profiles with two distinct sedimentation phases. Marked changes are observed in values of different sediment components, elemental concentrations and magnetic susceptibility in the two phases of sedimentation. Magnetic measurement and chemical analysis indicated an enrichment of magnetic particles and heavy metals in the upper portions of all the cores and decreasing pattern with depth suggesting that excess of anthropogenic loading occurred in the recent past. Increase in sedimentation rate in recent times is associated with increased deposition of finer sediment components, elements and magnetic minerals. The values of the different parameters analyzed in the present study therefore, depend, on one hand, on the amount provided by the parent material (lithogenic) and, on the other hand, on the extent of human impact (anthropogenic).

References

Ackermann, F., 1980. A procedure for correcting the grain-size effect in heavy metal analysis of estuarine and coastal sediments. Environmental Technology Letters 1, 518–527.

Agadi, V.V., 1986. Marine Algal Studies of the Central West Coast of India. Karnatak University 179 (Ph.D thesis).

Agarwal, J.M., 1990. Sea level variation-through bathymetric data example-Azhikkal on west coast of India. Sea Level Variation and Its Impact on Coastal Environment. Tamil university Press, Thanjavur, pp. 1–6.

Alagarsamy, R., 2009. Environmental magnetism and application in the continental shelf sediments of India. Marine Environmental Research 68, 49–58.

Alin, S.R., Cohen, A.S., 2003. Lake level history of Lake Tanganyika, East Africa, for the past 2500 years based on ostracode-inferred water depth reconstruction. Palaeogeography, Palaeoclimatology, Palaeoecology 199, 31–49.

Allen, J.R.L., Rae, J.E., Longworth, C., Hasler, S.E., Ivanonovich, M., 1993. A comparison of the ^{210}Pb dating technique with three other independent dating methods in an oxic estuarine salt-marsh sequence. Estuaries 16, 670–677.

Anderton, D.H.M., 1985. Sediments. In Historical Monitoring. Monitoring and Assessment Research centre, University of London 1–95.

Berner, R.A., 1980. Early Diagenesis: A Theoretical Approach. Princeton University Press, Princeton, New Jersey.

Blaha, U., Basavaiah, N., Deenadayalan, K., Borole, D.V., Mohite, R.D., 2011. Onset of industrial pollution recorded in Mumbai mudflat sediments, using integrated magnetic, chemical, ^{210}Pb dating, and microscopic methods. Environmental Science and Technology 45 (2), 686–692.

Bloemendal, J., King, J.W., Hall, F.R., Doh, S.J., 1992. Rock magnetism of Late Neogene and Pleistocene deep sediments: relationship to sediment source, diagenetic processes and sediment lithology. Journal of Geophysical Research 97, 4361–4375.

Borole, D.V., 1988. Clay sediment accumulation rates on the monsoon-dominated western continental shelf and slope region of India. Marine Geology 82, 285–291.

Borole, D.V., Sarin, M.M., Somayajulu, B.L.K., 1982. Composition of Narmada and Tapti estuarine particles and adjacent Arabian Sea sediments. Indian Journal of Marine Science 11, 51–62.

Bukhari, S.S., 1994. Studies on Mineralogy and Geochemistry of Bed and Suspended Sediment of Mandovi River and Its Tributaries in Goa, West Coast of India. Department of Marine Sciences, Goa University, Goa, India 240 (Ph.D. thesis).

Chan, L.S., Yeung, C.H., Yim, W.W.S., Or, O.L., 1998. Correlation between magnetic susceptibility and distribution of heavy metals in contaminated sea-floor sediments of Hong Kong Harbour. Environmental Geology 36, 77–86.

Chan, L.S., Ng, S.L., Davis, A.M., Yim, W.W.S., Yeung, C.H., 2001. Magnetic properties and heavy metal contents of contaminated seabed sediments of Penny's Bay, Hong Kong. Marine Pollution Bulletin 42, 569–583.

Crozaz, G., Picciotto, E., De Breuck, W., 1964. Antacric snow chronology with ^{210}Pb. Journal of Geophysical Research 69, 2597–2604.

Cundy, A.B., 1994. Radionuclide and Geochemical Studies of Recent Sediments from the Solent Estuarine System. Univ. Southampton, Southampton, UK (Ph. D. thesis).

Cundy, A.B., Croudace, I.W., 1995. Sedimentary and geochemical variations in a salt marsh/mudflat environment from the mesotidal Hamble Estuary, Southern England. Marine Chemistry 51, 115–132.

Das, P.K., Radhakrishna, M., 1993. Trends and the pole tide in Indian tide gauge records. Proceedings Indian Academy of Sciences (Earth Planetary Sciences) 102, 175–183.

Dekkers, M.J., 1989. Magnetic properties of natural pyrrohite. II. High and low temperature behaviour of Jrs and TRM as function of grain size. Physics of the Earth and Planetary Interiors 57, 266–283.

Dekkers, M.J., Passier, H.F., Schoonen, M.A.A., 2000. Magnetic properties of hydrothermally synthesized greigite (Fe_3S_4)-II. High and low-temperature characteristics. Geophysical Journal International 141, 809–819.

Deng, C.L., Zhu, R.X., Verosub, K.L., Singer, M.J., Yuan, B.Y., 2000. Paleoclimatic significance of the temperature-dependent susceptibility of Holocene loess, along a

Please cite this article as: Singh, K.T., et al., Changing environmental conditions in recent past — Reading through the study of geochemical characteristics, magnetic parameters..., Palaeogeography, Palaeoclimatology, Palaeoecology (2013), http://dx.doi.org/10.1016/j.palaeo.2013.04.008

NW–SE transect in the Chinese loess plateau. Geophysical Research Letters 27 (22), 3715–3718.
Desenfant, F., Petrovsky, E., Rochette, P., 2004. Magnetic signature of industrial pollution of stream sediments and correlation with heavy metals: case study from South France. Water, Air, and Soil Pollution 152, 297–312.
Dessai, D., Nayak, G.N., Basavaiah, N., 2009. Grain size, geochemistry and magnetic susceptibility: proxies in identifying sources and factors controlling distribution of metals in a tropical estuary, India. Estuarine, Coastal and Shelf Science 85, 307–318.
Fernandes, L., Nayak, G.N., 2009. Distribution of sediment parameters and depositional environment of mudflats of Mandovi estuary, Goa, India. Journal of Coastal Research 25 (2), 273–284.
Fernandes, L., Nayak, G.N., 2010. Sources and factors controlling the distribution of metals in mudflat sedimentary environment, Ulhas Estuary, Mumbai. Journal of Indian Association of Sedimentologists 29, 71–83.
Fernandes, L., Nayak, G.N., 2012a. Geochemical assessment in a creek environment: Mumbai, west coast of India. Environmental Forensics 13 (1), 45–54.
Fernandes, L., Nayak, G.N., 2012b. Heavy metals contamination in mudflat and mangrove sediments (Mumbai, India). Chemistry and Ecology 28 (5), 435–455.
Fernandes, L., Nayak, G.N., Ilangovan, D., Borole, D.V., 2011. Accumulation of sediment, organic matter and trace metals with space and time, in a creek along Mumbai coast, India. Estuarine, Coastal and Shelf Science 91, 388–399.
Flynn, W.W., 1968. The determination of low levels of ^{210}Po in environmental materials. Analytica Chimica Acta 43, 221–227.
Folk, R.L., 1968. Petrology of Sedimentary Rocks. Hemphills, Austin 177.
Froelich, P.N., Klinkhammer, G.P., Bender, M.L., Luedke, N.A., Heath, G.R., Cullen, D., Dauphin, P., 1979. Early oxidation of organic matter in pelagic sediments of the eastern equatorial Atlantic, suboxic diagenesis. Geochimica et Cosmochimica Acta 50, 1075–1090.
Gaudette, H.E., Flight, W.R., Toner, L., Folger, D.W., 1974. An inexpensive titration method for the determination of organic carbon in recent sediments. Journal of Sedimentary Petrology 44, 249–253.
Goddu, S.R., Appel, E., Jordanova, D., Wehland, F., 2004. Magnetic properties of road dust from Visakhapatnam (India)—relationship to industrial pollution and road traffic. Physics and Chemistry of the Earth 29, 985–995.
Grant, S.H., Middleton, R., 1990. An assessment of metal contamination of sediments in the Humber estuary, U.K. Estuarine, Coastal and Shelf Science 31, 71–85.
Higgitt, S.R., Oldfield, F., Appleby, P.G., 1991. The record of land use change and soil erosion in the late Holocene sediment of the Petit Lac d'Annecy, eastern France. The Holocene 1, 14–28.
IPCC, Inter Governmental Panel on Climate Change, 2007. The Physical science basis. Contribution of working group I to the fourth assessment report of the intergovernmental panel on climate change.
Jarvis, I.J., Jarvis, K., 1985. Rare earth element geochemistry of standard sediments: a study using inductively coupled plasma spectrometry. Chemical Geology 53, 335–344.
Jordanova, N., Jordanova, D., Tsacheva, T., 2008. Application of magnetometry for delineation of anthropogenic pollution in areas covered by various soil types. Geoderma 144, 557–571.
Kalesha, M., Rao, K.S., Somayajulu, B.L.K., 1980. Depositional rate in the Godavari Delta. Marine Geology 34, 57–66.
Kao, S.J., Horng, C.S., Roberts, A.P., Liu, K.K., 2004. Carbon–sulfur–iron relationships in sedimentary rocks from southwestern Taiwan: influence of geochemical environment on greigite and pyrrhotite formation. Chemical Geology 203, 153–168.
Karbassi, A.R., 1989. Geochemical and Magnetic Studies of Marine, Estuarine and Riverine Sediments near Mulki (Karnataka), India. Mangalore University, Mangalore 196 (PhD thesis).
Karlin, R., Lyle, M., Ross Heath, G., 1987. Authigenic magnetite formation in suboxic marine sediments. Nature 326, 490–493.
Klinkhammer, G.P., 1980. Early diagenesis in sediments from the eastern equatorial Pacific, II. Pore water metal results. Earth and Planetary Science Letters 49, 81–101.
Kumaran, K.P.N., Shindikar, M., Limaye, R.B., 2004. Mangrove associated lignite beds of Malvan, Konkan: evidence for higher sea level during the Late Tertiary (Neogene) along the West Coast of India. Current Science 86 (2), 335–340.
Laj, C., Kissel, C., Mazaud, A., Channell, J.E.T., Beer, J., 2000. North Atlantic palaeointensity stack since 75 ka (NAPIS-75) and the duration of the Laschamp event. Philosophical Transactions of the Royal Society of London 358 (1768), 1009–1025.
Lovley, D.R., Stolz, J.F., Nord Jr., G.L., Phillips, E.J.P., 1987. Anaerobic production of magnetite by a dissimilatory iron reducing microorganism. Nature 330, 252–255.
Lu, S.G., Bai, S.Q., 2006. Study on the correlation of magnetic properties and heavy metals content in urban soils of Hangzhou City, China. Journal of Applied Geophysics 60, 1–12.
Mackereth, J.H., 1966. Some chemical observations on post-glacial lake sediments. Philosophical Transactions of the Royal Society of London. Series 250 (B), 165–213.
Maher, B.A., Taylor, R.M., 1988. Formation of ultrafine grained magnetite in soils. Nature 336, 368–370.
Maher, B.A., Thompson, R., 1999. Quaternary Climates, Environments and Magnetism. Cambridge University Press, Cambridge.
Manjunatha, B.R., Shankar, R., 1992. A note on the factors controlling the sedimentation rate along the western continental shelf of India. Marine Geology 104, 219–224.
Naqvi, S.M., 2005. Geology and Evolution of the Indian Plate (from Hadean to Holocene — 4 Ga to 4 Ka). Capital publishing company, New Delhi 450.
Nayak, G.N., 1998. Impact of mining on Environment in Goa: a review. Environmental Geochemistry 1 (2), 97–100.
Nayak, G.N., 2002. Impact of Mining on Environment in Goa. international Publishers, India 112.
Nigam, R., Khare, N., Borole, D.V., 1991. Morphogroups of benthic foraminifera: proxy for Palaeomonsoonal precipitation. International Symposium on Oceanography of Indian Ocean. National Institute of Oceanography, Goa, p. 57.
Nigam, R., Khare, N., Nair, R.R., 1995. Foraminifera evidence for 77 year cycles of droughts in India and its possible modulation by the Gleissberg solar cycle. Journal of Coastal Research 11 (4), 1099–1107.
Oldfield, F., Yu, L., 1994. The influence of particle size variations on the magnetic properties of sediments from the north-eastern Irish Sea. Sedimentology 41, 1093–1108.
Petrovský, E., Kapicka, A., Jordanova, N., Boruvka, L., 2001. Magnetic properties of alluvial soils contaminated with lead, zinc and cadmium. Journal of Applied Geophysics 48, 127–136.
Reynolds, R.L., Tuttle, M.L., Rice, C.A., Fishman, N.S., Karachewskain, J.A., Sherman, D.M., 1994. Magnetization and geochemistry of greigite-bearing Cretaceous strata, North Slope basin, Alaska. American Journal of Science 294, 485–528.
Rijal, M.L., Appel, E., Petrovský, E., Blaha, U., 2010. Change of magnetic properties due to fluctuations of hydrocarbon contaminated groundwater in unconsolidated sediments. Environmental Pollution 158, 1756–1762.
Roberts, A.P., 1995. Magnetic properties of sedimentary greigite (Fe_3S_4). Earth and Planetary Science Letters 134, 227–236.
Sangode, S.J., Vhatkar, K., Patil, S.K., Meshram, D.C., Pawar, N.J., Gudadhe, S.S., Badekar, A.G., Kumaravel, V., 2010. Magnetic susceptibility distribution in the soils of Pune Metropolitan Region: implications to soil magnetometry of anthropogenic loading. Current Science 98, 516–527.
Sardesai, J.B., 1985. Mining industry and environmental erosion in Goa. Earth resources for Goa's development, pp. 424–429.
Sharma, P., Borole, D.V., Zingde, M.D., 1994. 210-Pb geochronology and trace element composition of the sediments in the vicinity of Bombay, west coast of India. Marine Chemistry 47, 227–241.
Shaw, T.J., Gieskes, J.M., Jahnke, R.A., 1990. Early diagenesis in differing depositional environments: the responses of transition metals in pore water. Geochimica et Cosmochimica Acta 54, 1233–1246.
Singh, K.T., Nayak, G.N., 2009. Sedimentary and geochemical signatures of depositional environment of sediments in mudflats from a microtidal Kalinadi estuary, Central west coast of India. Journal of Coastal Research 25 (3), 641–650.
Singh, K.T., Nayak, G.N., Fernandes, L.L., 2012. Geochemical evidence of anthropogenic impacts in sediment cores from mudflats of a tropical estuary, Central west coast of India. Soil and Sediment contamination 22 (3), 256–272.
Snowball, I.F., 1991. Magnetic hysteresis properties of greigite (Fe_3S_4) and a new occurrence in Holocene sediments from Swedish Lappland. Physics of the Earth and Planetary Interiors 68, 32–40.
Stoner, J.S., Channell, J.E.T., Hillaire-Marcel, C., 1995. Magnetic properties of deepsea sediments off southwest Greenland: evidence for major differences between the last two deglaciations. Geology 23, 241–244.
Swaminathan, H., 1982. Report of the Task Force on Eco-development Plan for Goa. Government of India, New Delhi 136.
Swart, D.H., 1983. Physical aspects of sandy beaches — a review. In: McLachlan, A., Erasmus, T. (Eds.), Sandy Beaches as Ecosystems. The Hague, The Netherlands-Junk, pp. 5–44.
Syvitski, J.P.M., Vo¨ro¨smarty, C.J., Kettner, A.J., Green, P., 2005. Impact of humans on the flux of terrestrial sediment to the Global Coastal Ocean Science. Science 308, 376–380.
Thompson, R., Oldfield, F., 1986. Environmental Magnetism. Allen & Unwin, London.
Torii, M., Fukuma, K., Horng, C.S., Lee, T.Q., 1996. Magnetic discrimination of pyrrhotite and greigite-bearing sediment sample. Geophysical Research Letters 23, 1813–1816.
Untawala, A.G., Dhargalkar, V.K., Agadi, V.V., Jagtap, T.G., 1979. Marine algal resources of the Maharashtra coast. Technical Report. National Institute of Oceanography, Goa, pp. 1–48.
Venkatachalapathy, R., Veerasingam, S., Basavaiah, N., Ramkumar, T., Deenadayalan, K., 2011. Environmental magnetic and petroleum hydrocarbons records in sediment cores from the north east coast of Tamilnadu, Bay of Bengal, India. Marine Pollution Bulletin 62, 681–690.
Wang, Y., Yang, Z., Shen, Z., Tang, Z., Niu, J., Gao, F., 2011. Assessment of heavy metals in sediments from a typical catchment of the Yangtze River, China. Environmental Monitoring and Assessment 172, 407–417.
Zhang, W., Yu, L., Hutchinson, S.M., 2001. Diagenesis of magnetic minerals in the intertidal sediments of the Yangtze Estuary, China, and its environmental significance. Science of the Total Environment 266, 169–175.
Zhang, W., Yu, L., Lu, M., Hutchinson, S.M., Feng, H., 2007. Magnetic approach to normalizing heavy metal concentrations for particle size effects in intertidal sediments in the Yangtze Estuary, China. Environmental Pollution 147, 238–244.
Zhang, C.X., Qiao, Q., Piper, J.D.A., Huang, B., 2011. Assessment of heavy metal pollution from a Fe-smelting plant in urban river sediments using environmental magnetic and geochemical methods. Environmental Pollution 159, 3057–3070.
Zwolsman, J.J.G., Berger, G.W., Van Eck, G.T.M., 1993. Sediment accumulation rates, historical input, post-depositional mobility and retention of major elements and trace metals in salt marsh sediments of the Scheldt Estuary, S.W. Netherlands. Marine Chemistry 44, 73–94.

Please cite this article as: Singh, K.T., et al., Changing environmental conditions in recent past — Reading through the study of geochemical characteristics, magnetic parameters..., Palaeogeography, Palaeoclimatology, Palaeoecology (2013), http://dx.doi.org/10.1016/j.palaeo.2013.04.008